Slope reversal of a monotonically decreasing electron tail in a strong magnetic field

I. Haber, J. D. Huba,[a] P. Palmadesso, and K. Papadopoulos

Naval Research Laboratory, Washington, D. C. 20375
(Received 2 November 1977)

An electron distribution with a long tail can be driven unstable by the resonant transfer of tail particle energy to electron cyclotron waves. The implications of this instability are examined by following its nonlinear evolution. The growth of wave energy can result in the formation of a positively sloped region of the electron distribution function. This positive slope causes a second mode to go unstable which subsequently results in large pitch angle diffusion of the tail particles.

I. INTRODUCTION

Plasma configurations involving a tenuous group of energetic electrons streaming along the ambient magnetic field abound both in laboratory experiments and in space. Such distributions have been experimentally measured in the auroral zones[1] while x-ray spectra indicate their presence in toroidal fusion machines[2] and solar flares.[3] The case where the distribution function of the field aligned energetic electrons has a positive slope is now a textbook matter.[4] In this case the collective effects quasi-linearly stabilize the beam plasma instability by flattening the positive slope,[4] although under some circumstances nonlinear effects prevent plateau formation.[5] In this paper we discuss the dynamics of the opposite effect. Namely, that in some parameter ranges, a monotonic field aligned distribution of energetic electrons can be transformed by collective effects into one with a positive slope. Since the positive slope which is formed can then drive numerous plasma instabilities, this process can be the key in explaining several of the mysteries observed in the operation of toroidal machines in the low density regimes[2,6-8] as well as a host of auroral[9] and solar flare phenomena.[3] The emphasis of this paper is understanding the fundamental physical phenomena, while the various applications will be discussed elsewhere.

II. THEORETICAL CONSIDERATIONS

Consider a model electron distribution function of the type

$$f_e(v) = f_M(v^2) + \alpha f_M(v_\perp^2) F(v_\parallel)\,, \tag{1}$$

where f_M is a Maxwellian with thermal velocity V_e, α is the relative tail density ($\alpha \ll 1$), and $F(v_\parallel)$ is given by

$$F(v_\parallel) = \begin{cases} 1/v_0, & 0 < v_\parallel < v_0\,, \\ 0, & \text{otherwise}\,, \end{cases} \tag{2}$$

with $v_0 \gg V_e$. The energy anisotropy of the long tail can drive electron cyclotron plasma waves unstable through a transfer of energy from particles to waves at the anomalous Doppler resonance,[10] $(\omega_k + \Omega_e)/k_\parallel = v_\parallel$, where $\Omega_e = |e|B/m_e c$ is the electron cyclotron frequency. For the case $\Omega_e \gg \omega_e$, the frequency of these waves is given by

$$\omega_k = \omega_e (k_\parallel / k) \tag{3}$$

while the growth rate is

$$\gamma_k = -\frac{\omega_k \mathrm{Im}\, D(k,\omega)}{2} = \frac{\pi\alpha}{2}\,\frac{\omega_k^3}{2\Omega_e |k_\parallel|}\left[-\frac{1}{\alpha} f_M'\left(\frac{\omega_k}{k_\parallel V_e}\right) + F\left(\frac{\omega_k + \Omega_e}{k_\parallel}\right) - \frac{k_\parallel V_e^2}{2\Omega_e} F'\left(\frac{\omega_k + \Omega_e}{k_\parallel}\right) - F\left(\frac{\omega_k - \Omega_e}{k_\parallel}\right)\right], \tag{4}$$

where $\omega_e = (4\pi n e^2/m_e)^{1/2}$ is the electron plasma frequency.

It is worth noting the physical significance of the terms involved in Eq. (4). While the derivation was for a distribution function as shown in Eq. (2), it is important to note that this result is valid for any distribution function with a long flat tail. The first term is the usual Landau damping term. The second is wave growth due to energy transfer at the anomalous Doppler resonance ($n = -1$), while the fourth is wave damping due to particles at the normal Doppler resonance ($n = +1$). The third term is the $n = -1$ Doppler shifted Landau damping. It is not significant initially, but can become important in later stages of the instability. It is easy to see that for the $\omega_k < \Omega_e$ and the distribution given by Eqs. (1) and (2),

$$F\left(\frac{\omega_k + \Omega_e}{k_\parallel}\right) \gg F\left(\frac{\omega_k - \Omega_e}{k_\parallel}\right)$$

so that the instability condition becomes

$$F\left(\frac{\omega_k + \Omega_e}{k_\parallel}\right) > \frac{1}{\alpha} f_M'\left(\frac{\omega_k}{k_\parallel V_e}\right) \tag{5}$$

subject to the constraint that there are particles at the velocities $(\omega_k + \Omega_e)/k_\parallel$, i.e.,

$$(\omega_k + \Omega_e)/k_\parallel < v_0\,. \tag{6}$$

Exact stability criteria can be numerically computed from inequalities (5) and (6). For our purposes it is worth noting that for $\omega_k \ll \Omega_e$, inequality (6) implies $k_\parallel > \Omega_e/v_0$, while inequality (5) implies $k_\parallel < \omega_e/v_1$ where v_1 satisfies the equation

[a] Present address: Science Applications, Inc., McLean, Va. 22101.

 0031-9171/78/2106-1013$00.90

$$F\left(\frac{\Omega_e}{k_\parallel}\right) = \frac{1}{\alpha} f'_M\left(\frac{v_1}{V_e}\right);$$

therefore, we have

$$\Omega_e/v_0 < k_\parallel < \omega_e/v_1 . \tag{7}$$

Condition (7) gives the range of wavelengths for which the growth rate is positive. It follows that the instability will exist only for

$$v_0/v_1 > \Omega_e/\omega_e . \tag{8}$$

Note that for most reasonable parameters $v_1 \approx 3V_e$.

Before proceeding to the simulations we comment on the expected nonlinear evolution. It can be shown by considering the detailed particle orbits that the interaction leads to pitch angle scattering for particles in resonance with the $n = -1$ Doppler shifted resonance. Since these particles are pitch angle scattered with a resulting decrease in their $v_\parallel$, they also lose energy to the wave fields. However, only those particles in resonance with the unstable waves, i.e., with $v_\parallel = (\Omega_e + \omega_k)/k_\parallel$ are affected. For the range of unstable $k_\parallel$ in Eq. (8) this implies

$$v_\parallel > (\Omega_e/\omega_1)v_1 \equiv v_2 . \tag{9}$$

As a consequence of the lack of diffusion for parallel velocities less than v_2 there is a tendency of particles to pile-up around v_2 and form a positive slope in $F(v_\parallel)$.

An additional effect is worth mentioning. The predominance of pitch angle scattering is only for particles which are Doppler resonant with the waves. For particles resonant at the phase velocity $v_\parallel = \omega_k/k_\parallel$ the predominant effect is a change in the parallel component of v, with the perpendicular component largely unaffected. Thus, particles which are pitch angle scattered then diffuse in velocity space due to a second wave driven unstable by the positive slope. The total effect will be pitch angle scattering over large angles. This effect is illustrated by the simulations.

III. COMPUTER SIMULATIONS

In order to determine the nonlinear evolution of the instability and check some of the conclusions of the preceding section and of Refs. 11 and 12 we carried out a series of numerical particle simulations. The simulations were run on an electrostatic particle code with one spatial direction and three velocity components. In order to have good statistics in the tail region, approximately 350 tail particles per cell were used in the simulation. This was four times as many as were used to simulate the main body Maxwellian. The simulations were performed along the linearly most unstable direction which was at an angle 55° to the magnetic field, $k_\parallel/k_\perp = \sqrt{2}/2$. The parameters used were $n_t/n_0 = 0.3$, $\Omega_e/\omega_e = 2$. The particles at the end of the tail had a velocity of 10 cells/ω_{pe} and the time step chosen was $\Delta t = 0.2\omega_{pe}^{-1}$. The reason for using rather large values of n_t/n_0 and ω_e/Ω_e was computational efficiency since the growth rate is proportional to n_t/n_0. A very low thermal velocity of $V_e = 0.02\ V_m$ was also chosen for efficiency of computation.

The initial velocity distribution $f(v_\parallel) = f(v)dv_\perp$ of the tail particles for the first simulation is shown in Fig. 1(a) along with a plot of number density in $v_x - v_y$ space [Fig. 1(b)]. Note that k is along the x axis so that the parallel direction is at an angle of 55° from x in Fig. 1(b). The numerical system used was 32 cells long. This was chosen so that the system would evolve in two separate stages to illustrate the physical processes responsible for the evolution of the distribution function.

The wavenumbers allowed in such a system are given as

$$k = (2\pi n/32), \quad n = 1, \ldots, 16 \tag{10}$$

The tick marks along the x axis in Fig. 1(a) represent the resonant velocities corresponding to various mode numbers and cyclotron harmonics. For example, the $(-1, 3)$ mode corresponds to a k of $6\pi/32$ and the anomalous Doppler shifted cyclotron resonance. The $(-1, 2)$ and $(-1, 1)$ modes are in regions of no particles as are the $(1, n)$ modes. The system was chosen so that the $(0, 1)$ mode is not too close to the fastest growing unstable mode, $n = 3$.

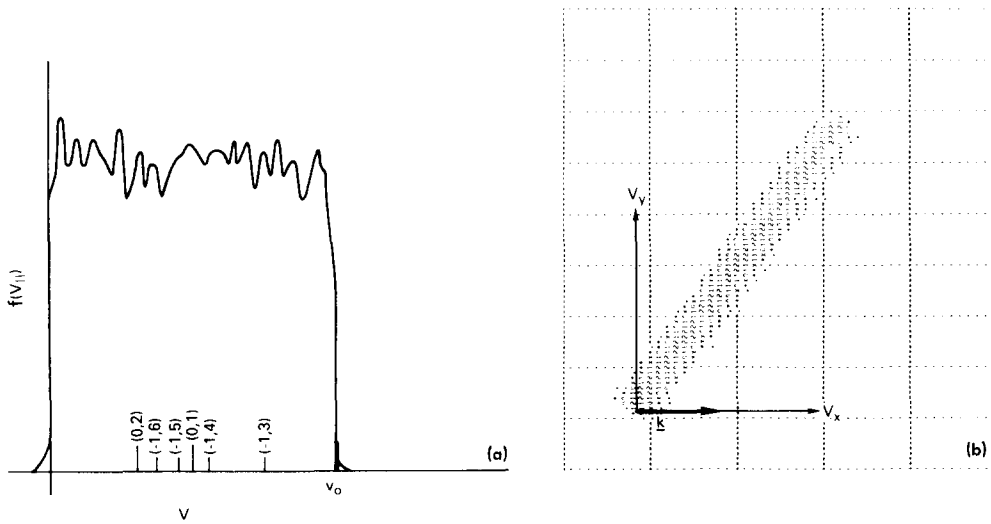

FIG. 1. Initial distribution of tail particles. (a) Distribution function parallel to B of tail particles only. Marks on the horizontal axis show the resonant velocities of various modes. The first index is the cyclotron harmonic number, the second is the wave number in units of the reciprocal length of the numerical system. (b) Distribution of tail particles in V_x-V_y space.

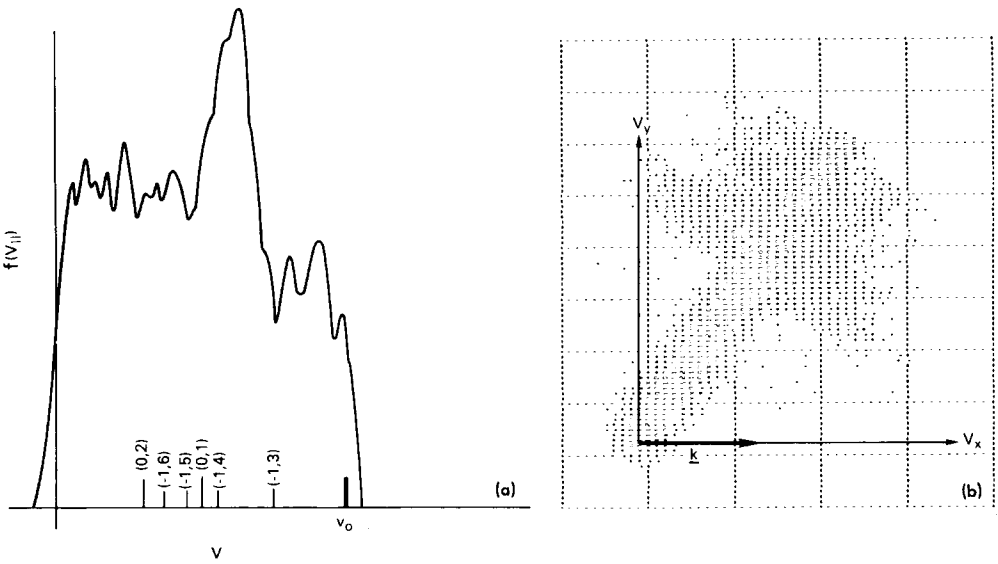

FIG. 2. Distribution of tail particles after 600 ω_e^{-1}. (a) Parallel distribution function of tail particles showing the formation of a positively sloped region near the (-1, 3) resonant velocity. (b) V_x-V_y distribution function of tail particle showing the pitch angle scattering in the resonant region.

The growth rate is proportional to $1/k_{\parallel}$ and therefore to $1/n$ so that the behavior of the system is initially dominated by a single mode.

Figure 2(a) shows the parallel velocity distribution after 600 ω_{pe}^{-1}. The formation of a positively sloped region is clearly evident in the region of the $(-1, 3)$ resonant velocity.

Figure 3(a) shows the time history of mode 3 indicating it has reached saturation. In this particular instance, saturation is primarily due to a decrease in the $F(\omega_e + \Omega_e/k_{\parallel})$ term in Eq. (4) (to about 20% of its initial value) and the Doppler shifted Landau damping caused by the large negative slope generated by the pitch angle scattered particles. Some decrease in the growth rate is also likely because of a flattening of $\partial F/\partial v_{\perp}$ and finite Larmor radius effects, but these are not as significant for the parameters used.

It should be noted in Fig. 2(a) that the positively sloped region generated by pitch angle scattering at the $(-1, 4)$ resonance is approaching the (0, 1) resonant velocity and the $n = 1$ mode should then go unstable. This is indeed seen to be the case in Fig. 3(b) which shows that the $n = 1$ mode has started to grow. A noticeable effect is that the new nonlinearly generated instability has a growth faster than the original Doppler resonance one.

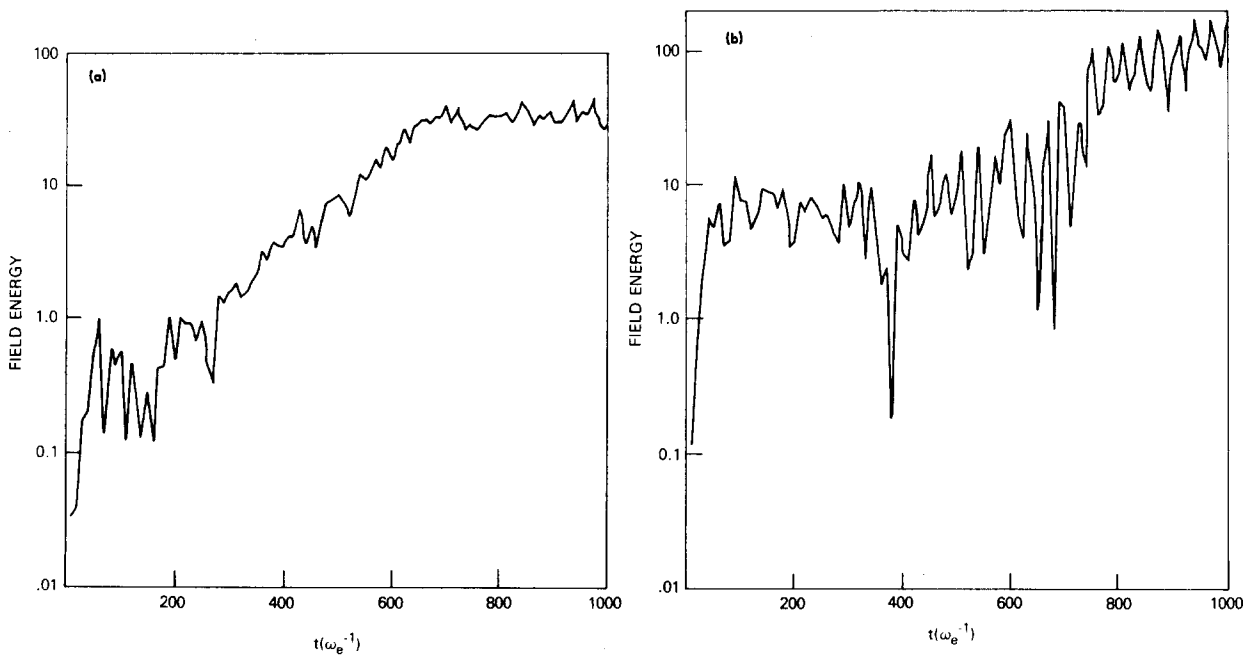

FIG. 3. Time evolution of $n = 1$ and $n = 3$ nodes. (a) Time evolution of the $n = 3$ mode energy showing exponential growth and then saturation around 700 ω_e^{-1}. (b) Time evolution of the $n = 1$ mode energy showing the growth of the Landau mode driven unstable because of the positive slope in the distribution function.

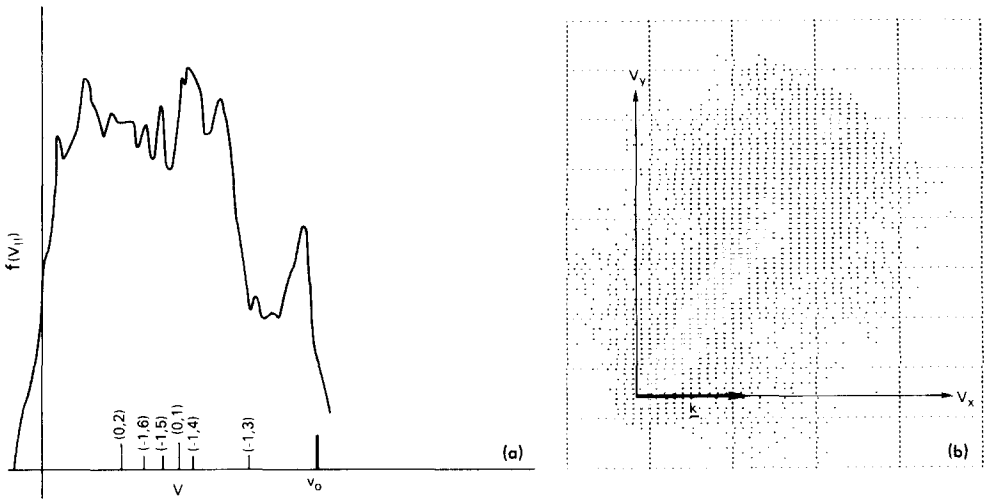

FIG. 4. Distribution of tail particles after 900 ω_e^{-1}. (a) Parallel distribution of the tail particles showing the quasi-linear flattening of the distribution function by the $n=1$ mode. (b) V_x-V_y distribution of tail particles showing the large angle scattering caused by the $n=1$ mode growth.

Figure 4(a) shows the distribution function at $t=900$ ω_{pe}^{-1} after the $n=1$ mode has saturated. The quasi-linear flattening of the distribution function is evident. More important, Fig. 4(b) shows the distribution function at the same time in V_x-V_y space. Note how the parallel velocities of the resonant particles have been decreased resulting in some particles with large $v_\perp/v_\parallel$. Since these particles started with large $v_\parallel/v_\perp$, they have been pitch angled scattered close to 90°.

An actual physical system is likely to exhibit a complicated competition amongst the various effects outlined. In particular, the competition between the tendency of pitch angle scattering to form a positively sloped region and the quasi-linear flattening of this region by modes driven unstable will be much less clearly defined. To illustrate this a computer run on a system four times as long and containing four times as many particles was run. The same tendency toward isotropization of the distribution function by a combination of pitch angle scattering and quasi-linear flattening can be identified. However, the isolation of the two effects is somewhat more difficult. This will be especially true in two and three dimensions. However, the basic physics is still unchanged.

IV. CONCLUSION

We have illustrated how it is possible for a long tailed distribution function, of the type which can be formed by large electric fields, to relax toward isotropy via a two stage process. First, a positively sloped region is formed by energy exchange at the anomalous Doppler resonance and second, this slope drives other instabilities. The actual occurrence of this scenario should be accompanied by radiation from the instability fields and from the pitch angle scattered particles. Radiation should also occur as a result of any subsequent instabilities driven by the positive slope, and it has been shown that these instabilities can form tails in the ion distribution function with large perpendicular velocities. In addition, the particles can be trapped in local variations of the ambient magnetic field. There is considerable experimental evidence for the actual existence of these effects and they have recently been discussed by Liu *et al.*[8]

ACKNOWLEDGMENTS

This work was supported by the Energy Research and Development Administration, Contract E(49-20)-1006. One of us (JDH) was a National Research Council-Naval Research Laboratory Research Associate during the course of this research.

[1]K. Papadopoulos and T. Coffey, J. Geophys. Res. **79**, 674 (1974).
[2]G. Boxman, B. Coppi, L. C. J. M. deKock, B. J. H. Meddens, A. A. M. Oomens, L. Th. M. Ornstein, D. S. Pappas, R. R. Parker, L. Pieroni, S. E. Segre, F. C. Schuller, and R. J. Taylor, in *Proceedings of the Seventh European Conference on Plasma Physics* (Centre de Recherches en Physique des Plasmas, Ecole Polytechnique Federal de Lausanne, Lausanne, Switzerland, 1975), Vol. II, p. 14.
[3]Z. Svestka, *Solar Flares* (Reidel, Dordrecht, Holland, 1975).
[4]R. C. Davidson, *Methods in Nonlinear Plasma Theory* (Academic, New York, 1972).
[5]K. Papadopoulos, Phys. Fluids **18**, 1769 (1975).
[6]TFR Group, in *Plasma Physics and Controlled Nuclear Fusion Research* (International Atomic Energy Agency, Vienna, 1975), Vol. I, p. 135.
[7]C. S. Liu and Y. C. Mok, Phys. Rev. Lett. **38**, 162 (1977).
[8]C. S. Liu, Y. C. Mok, K. Papadopoulos, F. Engelmann, and M. Bornatici, Phys. Rev. Lett. **39**, 701 (1977).
[9]D. A. Gurnett, L. A. Frank, and R. P. Lepping, J. Geophys. Res. **81**, 3059 (1976).
[10]B. B. Kadomtsev and O. P. Pogutse, Zh. Esp. Teor. Fiz. **53**, 2025 (1967) [Sov. Phys.-JETP **26**, 1146 (1968)].
[11]K. Papadopoulos, B. Hui, and N. Winsor, Nucl. Fusion **17**, 1087 (1977).
[12]B. Basu, B. Coppi, K. Molvig, F. Pegoraro, I. Haber, B. Hui, P. Palmadesso, K. Papadopoulos, and N. Winsor, in *Plasma Physics and Controlled Nuclear Fusion Research*, Berchtesgaden (International Atomic Energy Agency, Vienna, 1977), Vol. II, p. 455.